Elastic and anelastic properties of densified vitreous B₂O₃: Relaxations and anharmonicity

Giovanni Carini Jr.,[1] Giuseppe Carini,[2,*] Gaspare Tripodo,[2] Gaetano Di Marco,[1] and Edmondo Gilioli[3]

[1]*IPCF del C.N.R., Sezione di Messina, Viale Ferdinando Stagno d'Alcontres 37, I-98166 Messina, Italy*
[2]*Dipartimento di Fisica, Università Degli Studi di Messina, Viale Ferdinando Stagno d'Alcontres 31, I-98166 Messina, Italy*
[3]*IMEM del C.N.R., Area delle Scienze, I-43010 Parma, Italy*

The elastic and anelastic properties of densified B₂O₃ glasses, melt quenched under pressures of 2 and 4 GPa, were investigated by measuring the sound velocity and the acoustic attenuation of longitudinal and shear ultrasonic waves in the megahertz range over the temperature interval between 8 and 300 K. Densification from 1826 to 2373 kg/m³ leads to an extraordinarily large growth of both bulk and shear moduli but leaves the Poisson's ratio nearly constant. In the glass compacted at 4 GPa, the elastic moduli become larger by a factor of five than those characterizing normal vitreous B₂O₃ (v-B₂O₃) as a consequence of modifications of the chemical bonding in the network. The thermally activated relaxations of intrinsic structural defects, which dominate the acoustic behaviors of normal glass below 150 K, giving rise to an intense attenuation peak and a corresponding steep decrease in sound velocity, are increasingly depressed by growing densification. Above 150 K, the ultrasonic velocity is mainly regulated by the vibrational anharmonicity and shows a nearly linear decrease as the temperature is increased, with a substantially smaller slope with increasing densification. Modeling the relaxation losses and the related velocity variations by an asymmetric double-well potential model that has a distribution of both the barrier potential and the asymmetry, it has been possible to separate the relaxation and the anharmonic contributions to the sound velocity. The former has been ascribed to local motions of boroxol rings formed by connected BO₃ planar triangles, the basic units building up the network of v-B₂O₃, while the latter has been interpreted in terms of the Akhiezer mechanism concerning the "thermal vibration viscosity."

I. INTRODUCTION

Sound propagation in amorphous solids is regulated by distinct and competing mechanisms, whose relative contributions depend on the temperature and frequency ranges explored. Over the wide frequency range from hertz to gigahertz, it is well established that the acoustic behaviors of oxide glasses are mainly determined by (1) local motions of intrinsic structural defects—i.e., by tunneling at low temperatures ($T < 10$ K) and classical activation at higher temperatures ($T > 10$ K)—and (2) vibrational anharmonicity regulating the interactions between sound waves and thermal vibrations.[1–5] The former causes an increase of the acoustic attenuation (equivalently, the internal friction Q^{-1}) at the lowest temperatures, followed by a temperature-independent plateau and then by a well-pronounced peak and the associated variations of sound velocity. The latter becomes efficient in the temperature region above 100 K, where the mean free path of thermal modes is shorter than the acoustic wavelength. In particular, it has been shown[4,5] that the Akhiezer mechanism of "phonon viscosity" dominates the hypersonic attenuation in the region of temperatures above the attenuation peak while giving a negligible contribution at lower frequencies (from hertz to megahertz). In addition, it regulates the linear decrease in sound velocity over the whole frequency range in glasses that do not have a tetrahedrally coordinated network.[3–8]

The relation between disordered topology and defect modes can be explored in amorphous solids whose density is increased without altering their stoichiometry. This can be obtained by "hot" densification of a glass—i.e., by quenching the melt of a glass-forming liquid subjected to high pressures in the gigapascal range. Because the structure of "hot" densified glasses reflects the one of the supercooled liquid at high pressure at the glass transition temperature T_g, remarkable modifications of the short- and medium-range orders leading to a reduction of the local atomic mobility are expected.

B₂O₃ glasses, permanently compacted by melt quenching under pressures between 1 and 5.8 GPa, disclosed substantial structural changes. Experiments of nuclear magnetic resonance[9] and Raman scattering[10] revealed that the increasing density of glass is associated with the decreasing fraction of boroxol rings and, for quenching pressures higher than 3.8 GPa, to the transformation of threefold coordinated boron atoms (B⁽³⁾) in fourfold coordinated borons (B⁽⁴⁾), whose number increases with increasing pressure.[9] Boroxol rings (B₃O₆) are the molecular groups formed by connected BO₃ planar triangles, which are the basic units building up the network of normal vitreous B₂O₃ (v-B₂O₃).[11,12] The change in cation coordination from three to four can be considered possible evidence for existence in the system of glassy polymorphs, which reflect the two crystalline forms of boron oxide:[13] low-density α-B₂O₃ and high-density β-B₂O₃, the former being trigonal and the latter tetrahedral.

In this paper, we report a study concerning the temperature dependence of the acoustic attenuation and sound velocity at megahertz frequencies in permanently compacted glassy B₂O₃. Our aim is to investigate the behavior with increasing density of the mechanisms governing sound propagation. The results prove that the decrease of boroxol rings and the appearance of tetra-coordinated boron atoms with increasing pressure of synthesis substantially enhance the elastic moduli and markedly depress the population of relaxing defects, also altering the anharmonicity of these glasses.

II. EXPERIMENTAL DETAILS

B_2O_3 glasses were prepared by melt quenching using, as starting material, laboratory reagent 99.999% purity grades of boron oxide isotopically enriched in ^{11}B (99%). Since boron oxide is quite hygroscopic and its elastic properties depend on OH content,[3] a glass (dry v-B_2O_3) that has a H_2O content of 210 ppm (furnished and certified by Alfa Aesar) was also prepared and used as a reference. They were annealed and stabilized using the same procedure described elsewhere.[10] Densification was obtained by loading $^{11}B_2O_3$ glasses in a multianvil high-temperature/high-pressure apparatus for synthesis at 2 and 4 GPa. They were fused under pressure at 1150 °C for ~10 min (2-GPa glass) and at 1200 °C for ~30 min (4-GPa glass) and then quenched at that pressure. A typical raw sample had a diameter and a length of ~4.5 mm. Both the normal and the compacted samples were clear and transparent, and they did not show any traces of internal cracks. Just after the synthesis and 1 year later, the densified B_2O_3 glasses were characterized by x-ray diffraction, which revealed no signs of crystallization.

The density was measured at room temperature by a Micromeritics AccuPyc 1330 gas pycnometer under helium gas that has an accuracy of 0.03%. The densities of normal and densified B_2O_3 glasses are 1826 kg/m^3 (normal), 2082 kg/m^3 (2 GPa) and 2373 kg/m^3 (4 GPa).

Longitudinal and shear sound waves were obtained by tuning X- and Y-cut quartz crystals at their fundamental frequency. The attenuation and velocity of longitudinal (V_l) and shear (V_t) waves were performed at 10 MHz via a pulse-echo technique as described in previous work.[14] The correct echo overlap for sound velocity measurements was obtained by using the ΔT McSkimin criterion.[15] The sample-transducer bonding agents were Dow Corning silicon fluid between 8 and 190 K and Apiezon N grease between 120 and 300 K. A correction to account for the bonding was not carried out, but a rough evaluation of the corresponding error introduced in the velocity gave a value of less than 0.1%. The thermal scanning between 8 and 300 K was carried out by using a cryogenerator. The thermostatic control was better than 0.1 K over the whole temperature range.

We want to emphasize that the short length of 4-GPa glass led to partial overlap of adjacent echoes from the specimen following the application of a pulse of longitudinal ultrasonic waves, preventing a reliable measurement of the very high sound velocity. In this case, V_l was determined by measuring

the velocity of shear waves and by using the value (1.77) of the ratio $\frac{v_{B,l}}{v_{B,t}} = \frac{V_l}{V_t}$ between the Brillouin frequency shifts $v_{B,i}$ of transverse and longitudinal acoustic modes observed in Brillouin light scattering (BLS) spectra. BLS spectra were measured at room temperature using a Sandercock tandem Fabri-Perot interferometer at the Physics Department of Perugia University, Italy. The spectra were measured at 90° scattering. This geometry provided the frequency shifts $v_{B,i}$ determined by light scattering from an acoustic wave of velocity V_i in a isotropic medium: $v_{B,i} = \frac{2nV_i}{\lambda_L} \sin(\frac{\theta}{2})$ ($\lambda_L = 532.0$ nm is the laser wavelength, the index i corresponds to transverse or longitudinal acoustic modes, and $\theta = 90°$ is the scattering angle).

The specific heat capacities of normal and densified samples were determined using a Pyris differential scanning calorimeter (DSC, PerkinElmer). Discs of each glass of mass of ~15 mg were encapsulated in aluminum pans and subjected to the same thermal cycles from 200 to ~840 K with a heating rate of 10 K/min. Calibrations of the DSC output were performed using a standard sapphire sample. The specific heat capacity data of normal v-B_2O_3 are in good agreement with those of Richet *et al.*,[16] measured by adiabatic calorimetry from ~5 to 350 K.

Thermal expansion measurements were made from 120 to 350 K using a Netzsch Industries silica linear variable differential transformer horizontal dilatometer with a heating rate of 2 K/min.

III. RESULTS AND DISCUSSION

A. Elastic moduli and Poisson's ratio

The rigidity of B_2O_3 glasses critically depends on densification: a density increase by 30% in 4-GPa glass leads to a very large growth of both bulk B ($= \rho V_l^2 - \frac{4}{3}G$) and shear G ($= \rho V_t^2$), moduli, which are larger by a factor of five than those characterizing normal v-B_2O_3 (Table I). Figures 1(a) and 1(b) show that the variations of the moduli vs quenching pressure in hot densified glassy B_2O_3 below 4 GPa are slightly larger than those revealed in SiO_2 and GeO_2 glasses compacted at temperatures below T_g,[17,18] with the value at 4 GPa exhibiting a sharp jump. This is because in cold densified glasses, for example, hot densification at pressures below 4 GPa causes only modifications of the medium-range order associated with the formation of more packed groups of atoms,[10] which give rise to a nearly linear increase of the elastic constants. In a 4-GPa glass, we instead have variations

TABLE I. Parameters of normal and densified B_2O_3 glasses. Room temperature values are given of the density ρ, longitudinal V_l and shear V_t sound velocities, Debye sound velocity V_D, bulk B and rigidity G moduli, Poisson's ratio ν, linear thermal expansion coefficient α_{th}, and average thermal Grüneisen parameter γ_{th}.

B_2O_3 glasses	ρ (kg m^{-3})	V_l (m s^{-1})	V_t (m s^{-1})	V_D (m s^{-1})	B (GPa)	G (GPa)	ν	α_{th} (10^{-6} K^{-1})	γ_{th}
Dry[a]	1829	3261	1786	1992	11.67	5.84	0.286	16.9	0.37
Normal	1826	3242	1830	2036	11.04	6.12	0.266	16.3	0.33
2 GPa	2082	3737	2141	2379	16.35	9.54	0.256	15.0	0.39
4 GPa	2373	6462[b]	3651	4061	56.91	31.63	0.266	5.69	0.49

[a]H_2O content: 210 ppm.
[b]Value obtained by the ultrasonic V_t and the ratio between the Brillouin frequency shifts of longitudinal and transverse acoustic modes observed in BLS spectra, $\frac{V_l}{V_t} = 1.77$.
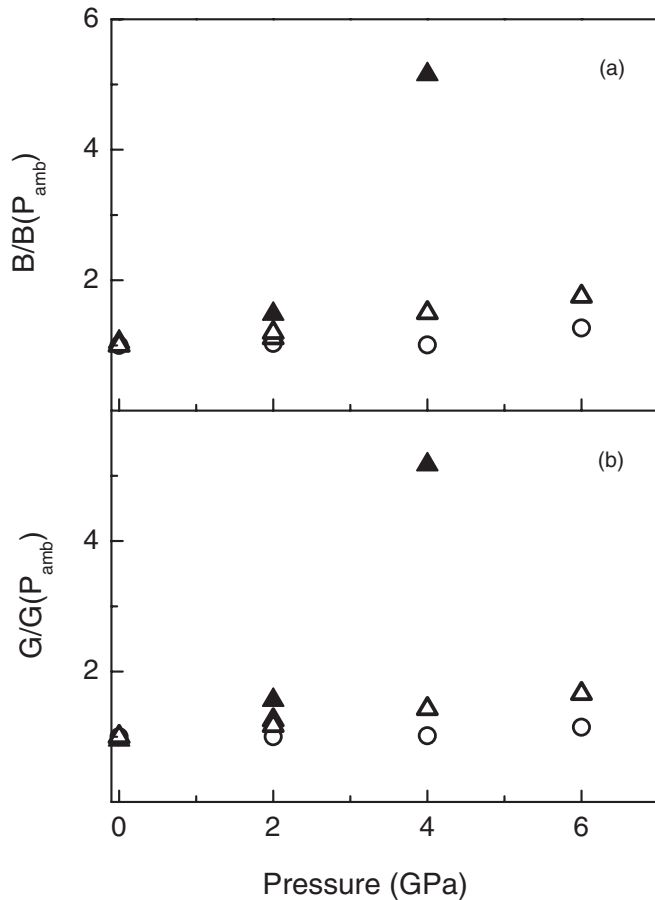
FIG. 1. Bulk (B) and shear (G) moduli normalized to ambient pressure values and plotted vs quenching pressure in glasses compacted at temperatures above (hot) and below (cold) T_g: (a) $B(P)$ in B_2O_3 (hot, present results, filled triangles), GeO_2 (cold, Ref. 17, open triangles), SiO_2 (cold, Ref. 18, open circles); (b) $G(P)$ in B_2O_3 (hot, present results, filled triangles), GeO_2 (cold, Ref. 17, open triangles), SiO_2 (cold, Ref. 18, open circles).

FIG. 2. (a) Poisson's ratios ν plotted vs quenching pressure in glasses compacted at temperatures above (hot) and below (cold) T_g: $\nu(P)$ in B_2O_3 (hot, present results, filled triangles), GeO_2 (cold, Ref. 17, open triangles), and SiO_2 (cold, Ref. 18, open circles). (b) Poisson's ratios ν at ambient pressure plotted vs average coordination number of NFIs in v-Se and v-As_2Se_3 (Ref. 20), v-B_2O_3 (present results), v-GeO_2 (Ref. 17), and v-SiO_2 (Ref. 18). The dotted line is a visual guide.

of the short-range order associated with the formation of tetra-coordinated boron atoms,[10] which increase the connectivity of the borate network (defined as the number of bridging bonds per network forming ion, or NFI) giving rise to the observed sharp stiffening.

Quite differently, the Poisson's ratio $\nu = \frac{V_l^2 - 2V_t^2}{2(V_l^2 - V_t^2)}$ shows a value of 0.266 in normal v-B_2O_3 and remains close to ~0.26 (Table I) in both compacted glasses independently of the quenching pressure Fig. 2(a). This behavior differs from the slight increase from 0.207 (at ambient pressure) to 0.22 (at 6 GPa) and from 0.168 (at ambient pressure) to 0.193 (at 6 GPa) experienced from cold densified GeO_2 and SiO_2 glasses, respectively; these values are included in Fig. 2(a) for comparison. *In situ* measurements on SiO_2 glass revealed a minimum at ~3 GPa ($\nu = 0.15$) and then an increase up to a value of 0.32 at 23 GPa, which remains about constant for even higher pressures.[19] As is well known, the Poisson's ratio is defined as the negative of the ratio of transverse to longitudinal strain, produced when a tensile loading is applied. Hence, it is expected that ν is strongly correlated to the connectivity of a glassy network, i.e., the larger the connectivity is and the

smaller ν becomes, because an increase of the bridging bonds per NFI causes increasing resistance to the shear deformation. This is clearly evidenced in Fig. 2(b), which reports the values of ν vs the average coordination number of NFI in prototype glasses that have a network essentially characterized by bridging bonds: the examined oxide glasses, v-Se ($\nu = 0.331$)[20] and v-As_2Se_3 ($\nu = 0.294$),[20] all quenched at ambient pressure. The increase of connectivity from 2 in v-Se, through 2.4 in v-As_2Se_3 and 3 in normal v-B_2O_3, to 4 in v-GeO_2 and v-SiO_2 is paralleled by a nearly linear decrease of ν.

The present observations prove that the variation of the medium- and short-range order obtained by hot compaction increases only slightly the resistance to the shear deformation of glassy B_2O_3. Despite a density variation of ~30%, a change of the atomic packing fraction Φ[21] from 0.35 in normal glass to 0.46 in 4-GPa glass, and the modifications of the chemical bonding in the network (i.e., the formation of tetra-coordinated boron atoms), the Poisson's ratio remains nearly constant. This behavior is quite different from that of v-SiO_2, whose ductility increases with increasing quenching or *in situ* applied pressure to values close to those of metals as a consequence of structural
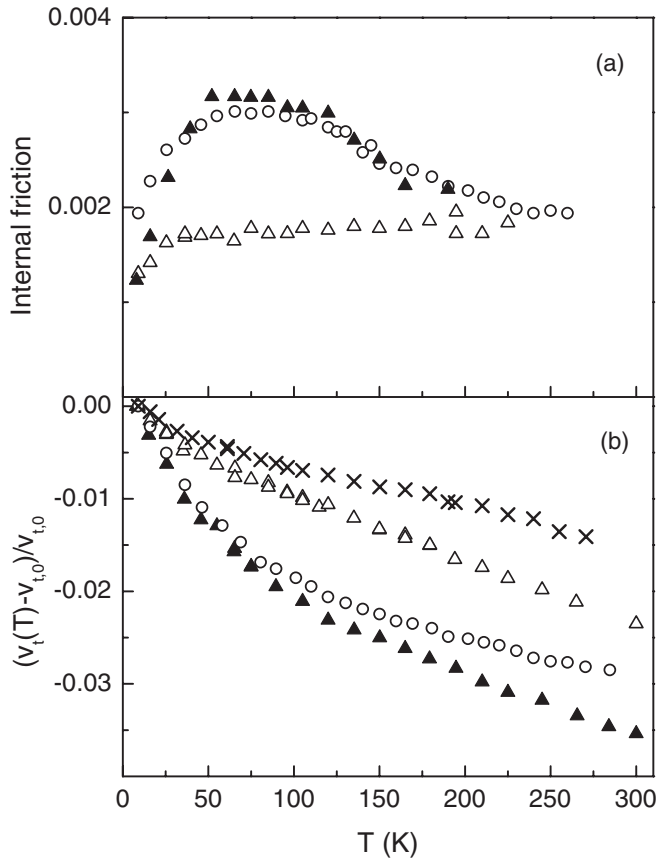
FIG. 3. (a) Comparison among temperature dependences of the internal friction Q^{-1} of 10-MHz shear ultrasonic waves in B$_2$O$_3$ glasses: dry (open circles), normal (filled triangles), and hot compacted at 2 GPa (open triangles). (b) Comparison among temperature dependences of the fractional sound velocities $\frac{V_t(T)-V_{t,0}}{V_{t,0}}$ of 10-MHz shear ultrasonic waves in B$_2$O$_3$ glasses: dry (open circles), normal (filled triangles), hot compacted at 2 GPa (open triangles), and hot compacted at 4 GPa (x).

rearrangements under pressure among different crystalline-like polymorphs.[19,23]

B. Acoustic attenuation and sound velocity

1. Analysis of ultrasonic data

Figure 3(a) compares the internal friction Q^{-1} of 10-MHz shear waves as a function of temperature between 8 and 300 K in dry, normal, and 2-GPa v-B$_2$O$_3$. The internal friction is related to the acoustic attenuation by the relation $Q^{-1} = 0.23 \frac{\alpha_{dB} V}{\omega}$, where α_{dB} is the attenuation in decibels per centimeter, V is the sound velocity, and ω is the angular frequency of ultrasonic waves. In both normal and dry v-B$_2$O$_3$, the internal friction shows very close temperature behaviors, exhibiting a broad peak $\sim$73 K, which is associated with thermally activated relaxations of structural defects over the potential barriers (in the schematic representation of defects by double-well potentials).[3] The loss peak is strongly depressed in 2-GPa glass, where the attenuation rises with increasing temperature to $\sim$40 K, becoming little dependent on temperature above 40 K.

In Fig. 3(b), the velocity of 10-MHz shear sound waves is shown as a function of temperature for dry, normal, and densified v-B$_2$O$_3$. The temperature dependences of the ultrasonic velocities in all the glasses studied show a negative temperature coefficient in the whole investigated range but with a larger slope at low temperatures. The shape of velocity curves between 8 and 120 K clearly indicates predominance of relaxation processes regulated by classical activation over potential barriers, while the nearly linear trend observed for higher temperatures is associated with the contribution of vibrational anharmonicity.[3] In agreement with the behaviors of acoustic loss, increasing densification depresses substantially the variation of $\frac{\Delta V_t}{V_{t,0}}$ between 8 and 120 K, indicating a parallel reduction of the relaxation strength. Moreover, the slope of the linear decrease observed at higher temperatures reduces appreciably by going from normal to 4-GPa v-B$_2$O$_3$.

The temperature behavior of the shear sound velocity V_t over the whole temperature range explored can be expressed by the following relation, which covers both relaxation and anharmonic contributions:

$$\frac{\Delta V_t}{V_{t,0}} = \left(\frac{\Delta V_t}{V_{t,0}}\right)_{rel} + \left(\frac{\Delta V_t}{V_{t,0}}\right)_{anh}, \qquad (1)$$

where $V_{t,0}$ is the sound velocity at the lowest temperature in the experiment and $\Delta V_t = V_t(T) - V_{t,0}$.

The relaxation term can be evaluated by the asymmetric double-well potential (ADWP) model.[24] In the ADWP model, the ultrasonic strain interacts with the population of intrinsic defects subjected to thermally activated local motions within ADWPs, having broad distributions of both the barrier height V and the asymmetry Δ: $g(V)$ and $f(\Delta)$. Modulation of the asymmetry Δ by a shear sound wave of angular frequency ω leads to a loss peak and a corresponding dispersion in the sound velocity when an appropriate interval of frequencies and/or temperatures is explored, because the relaxation time τ of defects is temperature dependent, $\tau = \tau_0 \exp(\frac{V}{k_B T}) \sec h(\frac{\Delta}{2k_B T})$. Using for $g(V)$ an exponential form, $g(V) = V_0^{-1} \exp(-\frac{V}{V_0})$, and taking $f(\Delta)$ as a constant f_0, the internal friction and the dispersion can be reduced to the following analytical expressions:[25,26]

$$Q_{rel}^{-1} = 2C_t^* \left[\frac{\alpha \pi/2}{\cos(\alpha \pi/2)} y_0^\alpha - \frac{\alpha}{1-\alpha} y_0 \right] \qquad (2)$$

$$\left(\frac{\delta V_t}{V_{t,0}}\right)_{rel} = C_t^* \left[\frac{\alpha \pi/2}{\sin(\alpha \pi/2)} y_0^\alpha - 1 \right], \qquad (3)$$

where $\alpha = \frac{k_B T}{V_0} = \frac{T}{T_0}$ and $y_0 = \omega \tau_0$. The relaxation strength is given by $C_t^* = \frac{\gamma_t^2 f_0}{\rho V_t^2}$, where γ_t is the deformation potential that expresses the coupling between the ultrasonic stress and the two-well systems and ρ is the sample density. Equations (2) and (3) account for the temperature dependences of Q_{rel}^{-1} and $(\frac{\delta V_t}{V_{t,0}})_{rel}$, with a negligible error in the megahertz range, and lead to a loss peak whose frequency and temperature dependences can be well approximated by the usual Arrhenius law that has V_0 as activation energy.

The anharmonic contribution $(\frac{\delta V_t}{V_{t,0}})_{anh}$ can be assessed by extending to glassy solids the theory concerning the interaction of sound waves with thermal phonons in dielectric crystals.[27,28] In the high-temperature region, the mean free

path of thermal modes is shorter than the acoustic wavelength and the condition $\omega\tau_{th} \ll 1$ is satisfied, where τ_{th} is the mean lifetime of thermal vibrations. This is the temperature region of the Akhiezer loss or phonon viscosity.[29] At ultrasonic frequencies, this condition is surely satisfied over the whole range of temperatures explored. Measurements of thermal conductivity Λ on v-B_2O_3[30] give a value of τ_{th} of 8.2×10^{-12} s at 8 K, a temperature that lies within the plateau region of Λ, where the dominant phonon approximation should be valid.[31]

Assuming a single value for τ_{th} in the temperature region where $\omega\tau_{th} \ll 1$, the acoustic loss and the variation of sound velocity are given by[4,5]

$$Q_{anh}^{-1} = A(T)\omega\tau_{th}, \quad \left(\frac{\delta V_t}{V_{t,0}}\right)_{anh} = -\frac{A(T)}{2}, \quad (4)$$

where $A(T) = \frac{\gamma_G^2 C_V T V_t}{2\rho V_D^3}$, γ_G^2 is the mean-square average Grüneisen parameter, C_V is the specific heat per unit volume, and V_D is the Debye velocity. In the ultrasonic range, the first part of Eq. (4) leads to a negligible acoustic loss, while the second one predicts a nearly linear temperature decrease for the sound velocity, in close agreement with the experimental behaviors observed in glasses that do not have a tetrahedrally coordinated network.[3,32]

Numerical evaluation of the ultrasonic relaxation loss (for $T \geqslant 8$ K) in normal v-B_2O_3 has been performed, obtaining a good fit of the experimental curve [solid line in Fig. 4(a)], with the following values for the relaxation parameters, also reported in Table II: $C_t^* = 2.3 \times 10^{-2}$, $T_0 = 820$ K, and $\tau_0 = 2 \times 10^{-14}$ s. By including these values in Eq. (3), it becomes possible to evaluate the relaxation contribution to the sound velocity; the resulting curve is reported in Fig. 4(b) as a solid line. By subtracting $(\frac{\delta V_t}{V_{t,0}})_{rel}$ from the experimental data, we obtain the curve labeled anh in Fig. 4(b). It shows a temperature decrease that becomes nearly linear above 150 K and reflects closely the behavior predicted by the mechanism of network viscosity [the second part of Eq. (4)], which is expected to cause measurable decreases of sound velocity only for temperatures higher than $\sim$20 K. These findings confirm that Eq. (1) represents the behavior of sound velocity over the whole temperature range explored and disclose that, above $\sim$200 K in this glass, the sound velocity can be expressed by the addition of a constant term, given by the relaxation strength C_t^*, and the anharmonic term $A(T)$, i.e., $(\frac{\delta V_t}{V_{t,0}})_{T\geqslant 200K} \cong -(C_t^* + \frac{A(T)}{2})$. This is because the first term in brackets on the right-hand side of Eq. (3) becomes increasingly negligible with increasing temperature and α. Combining the experimental values of $\frac{\delta V_t}{V_{t,0}}$ with the specific heats per unit volume C_V, the Debye velocities V_D, the shear velocities V_t, and the densities ρ, all of these quantities being measured at the same temperature of $\frac{\delta V_t}{V_{t,0}}$, it has been possible to estimate the average Grüneisen parameter γ_G^2 by the relation defining $A(T)$. The mean value of γ_G^2 obtained over the range between 200 and 300 K is 0.8 (corresponding to $\gamma_G = \pm0.89$).

Now we use the high-temperature limit of Eq. (1) to determine C_t^* and the average Grüneisen parameter γ_G^2 in densified glasses. By the values of $\frac{\delta V_t}{V_{t,0}}$ and of all physical parameters defining $A(T)$, measured over the interval between
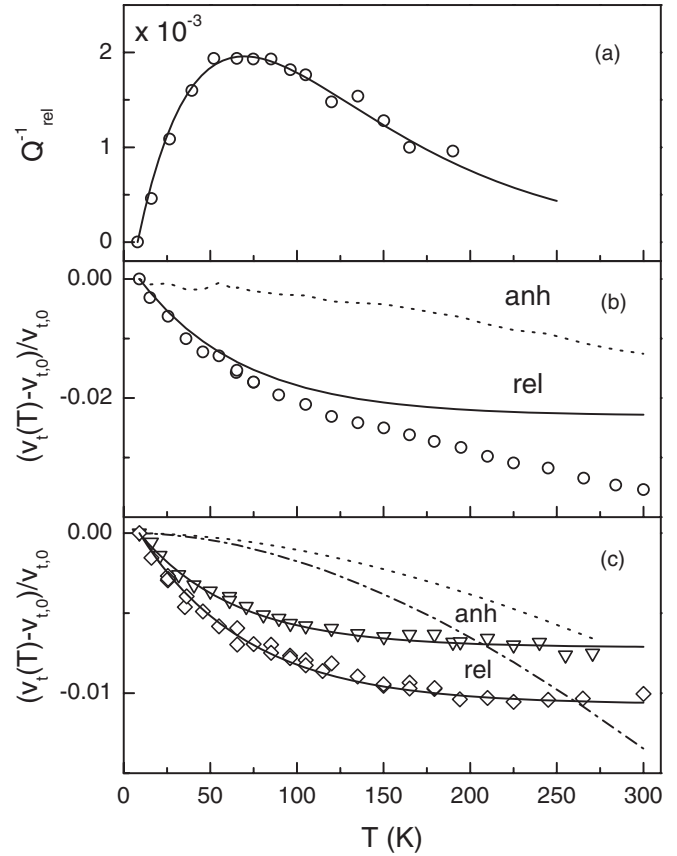
FIG. 4. (a) Comparison between experimental data of the relaxation loss Q^{-1}_{rel} at 10 MHz across the broad relaxation peak in normal v-B_2O_3 and the theoretical fit with the exponential distribution of activation energies by Eq. (2) (solid line). (b) Comparison among temperature dependences of the fractional sound velocity of 10-MHz shear ultrasonic waves in normal v-B_2O_3 (open circles), the relaxation contribution (solid line) evaluated by Eq. (3), and the anharmonic contribution (dotted line) given by the difference between the experimental data and the relaxation curve. (c) Temperature behaviors of anharmonic and relaxation contributions to the fractional sound velocity of 10-MHz shear ultrasonic waves in densified v-B_2O_3: 2-GPa glass, anharmonic (dash-dotted line), and relaxation (open diamonds), and 4-GPa glass, anharmonic (dotted line), and relaxation (open inverse triangles). The anharmonic contributions have been evaluated by Eq. (4), whereas the relaxation curves are the difference between experimental data and anharmonic behaviors. Solid lines represent the fit to the relaxation curves by Eq. (3).

200 and 300 K, we obtain $\gamma_G^2 = 1.24$ and $C_t^* = 0.0107$ for 2-GPa glass and $\gamma_G^2 = 2.39$ and $C_t^* = 0.0062$ for 4-GPa glass.

Assuming γ_G^2 as a constant over the whole temperature range explored and including in $A(T)$ the measured values of the other parameters, we obtain the temperature behaviors of $(\frac{\delta V_t}{V_{t,0}})_{anh}$ in both the densified glasses, which are reported as a dotted line and a dash-dotted line in Fig. 4(c). Within the experimental error, the measured specific heat capacities C_p of normal and densified B_2O_3 glasses are coincident over the interval between 200 and 500 K. This observation led us to use the values of C_p measured below 200 K in v-B_2O_3 by adiabatic calorimetry[16] for the compacted samples as well. Then, by subtracting $(\frac{\delta V_t}{V_{t,0}})_{anh}$ from the experimental values of $\frac{\delta V_t}{V_{t,0}}$, we

TABLE II. Values of the relaxation parameters in densified B_2O_3 glasses for relaxation strength C_t^*, activation energy V_0, characteristic time τ_0, coupling constant γ_t, and asymmetry distribution f_0.

B_2O_3 glasses	C_t^* (10^{-2})	V_0/k_B (K)	τ_0 $(10^{-13}$ s$)$	$f_0\gamma_t^2$ $(10^8$ J m$^{-3})$	γ_t (eV)	f_0 $(10^{46}$ J^{-1} m$^{-3})$
Normal	2.28	820	0.21	1.40	0.19	15.1
2 GPa	1.07	719	1.46	1.02	0.21	8.25
4 GPa	0.71	579	4.25	2.25	0.44	4.54

determine the relaxation contributions that are also shown in Fig. 4(c) as data points. Numerical evaluation of $(\frac{\delta V_t}{V_{t,0}})_{\rm rel}$ has been performed by Eq. (3) obtaining a good fit [solid line in Fig. 4(c)], and the values of relaxation parameters are included in Table II.

2. Anharmonicity

The obtained values of γ_G should be compared with those of the average thermal Grüneisen parameter $\gamma_{\rm th} = \frac{3\alpha_{\rm th}B^S V_m}{C_p}$ determined at room temperature (Table I). In this relation, $\alpha_{\rm th}$ is the linear thermal expansion coefficient, B^S is the adiabatic bulk modulus, V_m is the molar volume, and C_p is the molar heat capacity at constant pressure. The values of γ_G increase with increasing densification of glasses, in close agreement with the behavior observed for the thermal Grüneisen parameters $\gamma_{G,{\rm th}}$ (Table I). Low values of $\gamma_{\rm th}$ imply the presence of vibrational modes that have small or negative γ_G. Ultrasonic measurements under pressure on borate glasses[33] revealed that, in clear contrast with the positive values determined for the longitudinal acoustic-mode Grüneisen parameter $\gamma_{G,l}$, the values for the shear acoustic-mode Grüneisen parameter $\gamma_{G,t}$ are negative. In vitreous SiO_2, both the longitudinal and the shear acoustic-mode Grüneisen parameters are negative: the presence of vibrational modes that have negative γ_G has been explained by considering the open structure of this glass, which allows bending vibrations of oxygen atoms bridging between two silicon atoms.[34,35] This model emphasizes the importance of low-frequency transverse vibrations whose frequency increases with increasing volume. Low values of $\gamma_{\rm th}$ imply that bending vibrations could also play a significant role in the vibrational anharmonicity of v-B_2O_3.

3. Thermally activated relaxations

Inspection of the relaxation parameters reveals that the hardening of the elastic continuum due to compaction gives rise to a well-defined decrease of both the relaxation strength C_t^* and the apparent activation energy V_0. To consider the densification effect on the number of relaxing particles, we deduced the product $f_0\gamma_t^2$ from C_t^* (Table II). It decreases by going from normal v-B_2O_3 to 2-GPa glass, showing an unexpected marked increase in 4-GPa glass. It is believed that this increase mainly reflects a strong variation of γ_t^2, because it has been proved that the deformation potential increases roughly linearly with increasing glass transition temperature T_g.[36] The T_g of these glasses exhibits remarkable changes with hot densification at high pressures (from $\sim$533 K in v-B_2O_3, through 552 K in 2-GPa glass, to 748 K in 4-GPa glass), implying that the quantity in $f_0\gamma_t^2$, which increases with increasing densification, must be the deformation potential γ_t.

The deformation potentials deduced by linear interpolation from the plot of the values of γ_t vs T_g, experimentally determined in lithium borate glasses,[37] are reported, together with the obtained values of the spectral density of asymmetries f_0 in Table II. Assuming that $f(\Delta) = f_0$ below V_0 and $f(\Delta) = 0$ above V_0, the calculated number of relaxing particles decreases from an order of magnitude of 10^{27} m^{-3} in normal v-B_2O_3 to 10^{26} m^{-3} in 2- and 4-GPa glasses.

To discuss the possible microscopic origin of the relaxing centers, we have to distinguish between extrinsic and intrinsic defects, because v-B_2O_3 might contain a substantial amount of water or of OH^- hydroxyl ions. It has been found that the presence of OH^- groups has a large effect on some physical properties of glassy B_2O_3: they affect the high-temperature acoustic loss and the elastic characteristics,[38] giving rise to a hardening of the network, and the low-temperature specific heat capacity.[39] The data reported in Fig. 3 and Table I show that the behavior of the internal friction and the room temperature values of sound velocities and the expansion coefficient in normal v-B_2O_3 are close to those measured in the dry sample, which has a very low H_2O content (less than 0.1 mol% corresponding to a number of particles of $\sim$$10^{25}$ m^{-3}). Thus, it is reasonable to assume a similar number of OH groups in normal glass, which is used to synthesize the densified samples and, most importantly, to exclude these extrinsic defects as the origin of the observed relaxation processes.

The variations of both the relaxation strength and the activation energy V_0 should be attributed to relaxing particles whose local arrangement is significantly affected by structural modifications induced by network compaction. The absence of an adequate model describing the microscopic nature of defect states in glassy B_2O_3 leads us to try a possible explanation for the observed anelastic effects.

Recent Raman scattering measurements[10] revealed that the application of pressures to 4 GPa in the liquid phase of B_2O_3 gives rise to substantial variations of the connectivity of the glassy network, limiting the formation of boroxol rings during the next quenching process and causing the formation of pentaborate units, i.e., two boroxol rings linked by a tetra-coordinated boron atom. Melt quenching under pressure to 4 GPa of B_2O_3 hinders the transformation of BO_3 chainlike segments in rings during the cooling process, driving the system toward a glassy structure that has more efficient packing of the molecular units. Increasing density of the glass is associated with the decrease of the fraction of boroxol rings and with the enhancement of the network connectivity by variations in the chemical bonding. It is believed that both these modifications represent the source for the observed decrease of the number of relaxing units, the former preventing their local

mobility and the latter depressing their degrees of freedom. In this context, it is proposed that structural relaxations affecting the sound propagation in v-B_2O_3 originate from some kind of local motion of BO_3 groups connected to form the boroxol rings in the network. The present observations lead to the conclusion that glassy v-B_2O_3 that has a structure modified by increasing densification alters substantially the thermally activated local mobility as a consequence of substantial modifications of the short- and medium-range orders, which impose severe restrictions on the relaxing particles.

IV. CONCLUSIONS

An ultrasonic study of densified B_2O_3 glasses, melt quenched under pressures in the gigapascal range, has been performed over the temperature range between 8 and 300 K. In the glass compacted at the highest pressure (4 GPa), bulk and shear moduli become larger by a factor of five than those characterizing normal v-B_2O_3 as a consequence of modifications of the chemical bonding in the network (the formation of tetra-coordinated boron atoms). Quite differently, the Poisson's ratio remains nearly constant with increasing densification, despite variations of the short- and medium-range orders, which should hinder the local shear.

The analysis of the ultrasonic loss and sound velocity curves show that different dynamic mechanisms contribute to the sound propagation: (1) localized motion of structural defects and (2) vibrational anharmonicity. The locally mobile particles experience classical activation over potential barriers above 10 K. The relaxation strength C_i^* is found to be on the order of 10^{-2} and exhibits a well-defined decrease with increasing densification, which causes a significant reduction of the boroxol rings formed by connected BO_3 planar triangles, the basic units building up the skeleton of v-B_2O_3. These observations lead us to associate the defect states with some kind of local motion of BO_3 groups within boroxol rings. The evaluation of the relaxation contributions to the ultrasonic loss and sound velocity by the ADWP model permits us to assess the temperature behavior of sound velocity arising from the anharmonic interactions of thermal vibrations. This led to the quantitative evaluation of the mean acoustic-mode Grüneisen parameter γ_G in the temperature region where the acoustic behaviors should be governed by the Akhiezer mechanism of thermal vibration viscosity. The obtained values of γ_G exhibit an increase with increasing densification of glasses, in agreement with the behavior observed for the thermal Grüneisen parameters $\gamma_{G,th}$. These findings prove that, besides classical activation of structural defects, vibrational anharmonicity is playing a significant role in governing the sound velocity behavior in the megahertz range.

ACKNOWLEDGMENTS

*pino.carini@unime.it

[1] S. Rau, C. Enss, S. Hunklinger, P. Neu, and A. Würger, Phys. Rev. B **52**, 7179 (1995).

[2] K. A. Topp and G. Cahill, Z. Phys. B **101**, 235 (1996).

[3] G. Carini Jr., G. Carini, G. D'Angelo, G. Tripodo, A. Bartolotta, and G. Salvato, Phys. Rev. B **72**, 014201 (2005); G. Carini Jr., G. Carini, G. Tripodo, A. Bartolotta, and G. Di Marco, J. Phys. Condens. Matter **18**, 3251 (2006); G. Carini Jr., G. Carini, G. D'Angelo, G. Tripodo, A. Bartolotta, and G. Di Marco, J. Phys. Condens. Matter **18**, 10915 (2006).

[4] R. Vacher, E. Courtens, and M. Foret, Phys. Rev. B **72**, 214205 (2005).

[5] G. Carini Jr., G. Tripodo, and L. Borjesson, Phys. Rev. B **78**, 024104 (2008).

[6] G. Carini Jr., L. Orsingher, G. Tripodo, and E. Gilioli, Phil. Mag. **88**(33–35), 4143 (2008).

[7] J. Hertling, S. Baessler, S. Rau, G. Kasper, and S. Hunklinger, J. Non-Cryst. Solid. **226**, 129 (1998).

[8] S. Hunklinger and M. von Schickfus, in *Amorphous Solids*, edited by W. A. Phillips, Vol. 24 (Springer, Berlin, 1981), p. 81.

[9] V. V. Brazhkin, I. Farnan, K. I. Funakoshi, M. Kanzaki, Y. Katayama, A. G. Lyapin, and H. Saitoh, Phys. Rev. Lett. **105**, 115701 (2010).

[10] G. Carini Jr., E. Gilioli, G. Tripodo, and C. Vasi, Phys. Rev. B **84**, 024207 (2011).

[11] A. K. Hassan, L. M. Torell, L. Borjesson, and H. Doweidar, Phys. Rev. B **45**, 12797 (1992).

[12] P. Umari and A. Pasquarello, Phys. Rev. Lett. **95**, 137401 (2005).

[13] J. D. Mackenzie and W. F. Clausen, J. Am. Ceram. Soc. **44**, 79 (1961).

[14] G. Carini and F. Mento, J. Phys. E **12**, 259 (1979).

[15] E. P. Papadakis, *Physical Acoustics*, edited by R. N. Thurston and W. M. Mason (Academic, New York, 1976), Vol. XII, p. 277.

[16] P. Richet, D. de Ligny, and E. F. Westrum Jr., J. Non-Cryst. Solid. **315**, 20 (2003).

[17] L. Orsingher, M. Calicchio, Giovanni Carini Jr., R. Dal Mascio, D. Fioretto, E. Gilioli, M. Mattarelli, E. Moser, and F. Rossi., Phil Mag. **88**, 3907 (2008).

[18] M. Zanatta, G. Baldi, S. Caponi, A. Fontana, E. Gilioli, M. Krish, C. Masciovecchio, G. Monaco, L. Orsingher, F. Rossi, G. Ruocco, and R. Verbeni, Phys. Rev. B **81**, 212201 (2010).

[19] C.-S. Zha, R. J. Hemley, H. K. Mao, T. S. Duffy, and C. Meade, Phys. Rev. B **50**, 13105 (1994).

[20] N. Soga, M. Kunugi, and R. Ota, J. Phys. Chem. Solid. **34**, 2143 (1973).

[21] The packing fraction is defined as $\phi = \frac{N_A V_{\text{atomic}}}{V_{\text{molar}}}$, where V_{molar} is the molar volume and N_A is the Avogadro number. The theoretical ionic volume is given by $V_{\text{atomic}} = \sum \frac{4}{3}\pi r_i^3 X_i$, where r_i and X_i are the radius and the fraction, respectively, of the ith atom in the formula unit. The packing fractions for the studied glasses have been evaluated by the experimental values of density and ionic radii given by Shannon (Ref. 22) accounting for the typical coordinates characterizing the NFI in the examined glasses.

[22] R. D. Shannon, Acta Cryst. A **32**, 751 (1976).

[23]J. Hertling, S. Baessler, S. Rau, G. Kasper, and S. Hunklinger, J. Non-Cryst. Solid. **226**, 129 (1998).

[24]J. Jackle, L. Pichè, W. Arnold, and S. Hunklinger, J. Non-Cryst. Solid. **28**, 365 (1976).

[25]K. S. Gilroy and W. A. Phillips, Phil. Mag. B **43**(5), 735 (1981).

[26]J. P. Bonnet, J. Non-Cryst. Solid. **127**, 227 (1991).

[27]R. Truell, C. Elbaum, and B. B. Chick, *Ultrasonic Methods in Solid State Physics* (Academic Press, New York, 1969), p. 307.

[28]H. J. Maris, in *Physical Acoustics*, edited by W. P. Mason and R. N. Thurston, Vol. VIII (Academic Press, New York, 1971), p. 279.

[29]A. Akhiezer, J. Phys. USSR **1**, 1937 (1939).

[30]G. D'Angelo, C. Crupi, G. Tripodo, and G. Salvato, J. Phys. Chem. B **114**, 2467 (2010).

[31]T. Klitsner and R. O. Pohl, Phys. Rev. B **36**, 6551 (1987).

[32]T. N. Claytor and R. J. Sladek, Phys. Rev. B **18**, 5842 (1978).

[33]G. A. Saunders, H. A. A. Sidek, J. D. Comins, G. Carini, and M. Federico, Phil. Mag. **56**(1), 1 (1987).

[34]Y. Sato and O. L. Anderson, J. Phys. Chem. Solid. **41**, 401 (1980).

[35]G. K. White, S. J. Collocott, and J. S. Cook, Phys. Rev. B **29**, 4778 (1984).

[36]N. Reichert, M. Schmidt, and S. Hunklinger, Solid State Comm. **57**, 315 (1986).

[37]M. Devaud, J. Y. Prieur, and W. D. Wallace, Solid State Ionics **9-10**, 593 (1983).

[38]J. T. Krause and C. R. Kurkjian, in *Borate Glasses*, edited by L. D. Pye, V. D. Frechette, and N. J. Kreidl (Plenum, New York, 1978); Vol. 12, p. 577; J. T. Krause and C. R. Kurkjian, J. Am. Cer. Soc. **49**, 171 (1966).

[39]E. Perez-Enciso, M. A. Ramos, and S. Vieira, Phys. Rev. B **56**, 32 (1997).